Inversion of marine CSEM data using up-down wavefield separation and simulated annealing

Friedrich Roth[*] and Jürgen J. Zach, Electromagnetic Geoservices, Norway   (froth@emgs.com, jjz@emgs.com)

Summary

We demonstrate how processing data from shallow water CSEM surveys using up-down separation can improve the performance of a global inversion scheme. Data from a receiver over a known prospect produces a markedly improved reproduction of the resistivity profile in a plane-layer model employed for illustrative purposes. This improvement being particularly pronounced in the absence of a strong resistive anomaly, the results are directly applicable to finding starting models for more rigorous 3D inversion schemes as well as a to creating a reference model for Scanning survey interpretation.

Introduction

The 1D inversion of marine CSEM data is an easy way to generate depth-resistivity profiles required by more advanced data processing and interpretation schemes. Examples are the generation of starting models for rigorous 3D inversion or the interpretation of Scanning (i.e. reconnaissance) survey data (Wahrmund et al., 2006). The inversion of marine CSEM data is inherently ill-conditioned, in particular in shallow water (water depth < 500m), where the strong air wave dominates the measured electromagnetic field at large source-receiver offsets, thus masking the response from deeper resistors/hydrocarbon reservoirs (Roth and Maaø, 2007). Amundsen et al. (2006) introduced an effective method which attenuates the air wave and increases the sensitivity of marine CSEM methods by separating the measured wavefield into its up- and downward traveling constituents. Here we present example results from inverting shallow water CSEM data acquired offshore Norway using a simple 1D inversion scheme that combines the sensitivity enhancement of up-down wavefield separation with the global optimization capabilities of a simulated annealing (SA) search algorithm.

Up-down separation for air wave attenuation

Air wave attenuation by up-down separation takes advantage of the fact that the information about the subsurface is contained in the upward traveling constituent of the wavefield in the seafloor just below the CSEM receiver, whereas the air wave is traveling downward. Assuming a primarily vertically traveling wavefield, as is the case for large source-receiver offsets, the separation can be applied on a receiver-by-receiver basis using a simple linear combination of the measured electric and magnetic field components (see Amundsen et al., 2006):

$$E_x^{(U)} = 0.5\left(E_x - (i\omega\mu\rho_{SF})^{1/2} H_y\right),$$
$$H_y^{(U)} = -(i\omega\mu\rho_{SF})^{-1/2} E_x^{(U)} \tag{1}$$

Here, the superscript (U) denotes "upward", ρ_{SF} is the resistivity of the seafloor, ω is angular frequency, μ denotes the magnetic permeability, and $i = \sqrt{-1}$. Similar expressions exist for the upward constituents of E_y and H_x, respectively. The seafloor resistivity needs to be known a priori, however Roth and Maaø (2007) showed that the decomposition relation (1) is well-behaved and tends to enhance the sensitivity to resistive subsurface structures even when the assumed resistivity is incorrect. We therefore propose to use the same seafloor resistivity in the up-down separation as in the top-most layer of the inversion model. This approach renders the problem more non-linear as compared to keeping the resistivity fixed a priori, which favors the use of a global inversion scheme such as SA over gradient-based methods.

Simulating annealing

The technique of simulated annealing (SA) was invented in the early-mid 1980's (Kirkpatrick et al., 1983; Černy, 1985), based on the Metropolis algorithm (Metropolis et al., 1953), and has since become a tool in most fields of computational optimization. SA was applied to geophysical problems for the first time by Rothman (1985), and the method has since been successfully applied to several land CSEM (Sharma and Kaikkonen, 1998, Chunduru et al., 1996) and marine CSEM problems (Birsan, 2003; Routh and Oldenburg, 1999). The present study constitutes the first application of SA to the inversion of CSEM as acquired in a seabed logging (SBL) survey for hydrocarbon exploration.

Inversion scheme

The inversion considers a horizontally layered formation with layer resitivities initialized to the same value, e.g. 1 Ωm. The SA search loop (see figure 1) randomly draws new models based on a constrained Metropolis-type algorithm. New models are chosen under appropriate smoothness ($\Delta\rho < 50\Omega$m between neighboring layers) and absolute constraints (e.g. $\rho_{max} = 200\Omega$m). Since the resistivity of the uppermost layer (i.e. the seafloor) is used in the up-down separation, we adopted a stronger constraint here ($\rho_{SF,max} = 10\Omega$m). For each model, synthetic data are generated for E_x and H_y using an efficient quasi-analytical frequency-wavenumber domain code based on plane-wave decomposition (Løseth et al., 2006). The upward traveling wavefield is then extracted from both the synthetic and acquired data using equation (1), and a data misfit is computed. The misfit function ε shown in figure 1 is a simple deviation from unity of the synthetic normalized with the measured data F_{synt}/F_{meas} (F= $E_x^{(U)}, H_y^{(U)}$). Normalization also occurs with the number of source points (times number of frequencies times number of field components), N(Tx) (Tx for transmission points). The

Inversion of marine CSEM data using up-down wavefield separation and simulated annealing

natural logarithm, which is optional, is used in the following examples. Other misfit functions are, however, also investigated. Depending on the change of the misfit function, the new model can be either accepted as positive ("exothermic" step) or accepted with a Boltzmann-probability of $P=\exp(-\Delta\varepsilon/T)$ as negative ("endothermic" step). The temperature is lowered according to an exponential cooling schedule, whereas different cooling strategies were investigated. Stopping criteria are either the inversion being idle for a preset number of iterations (usually a few hundred), upon which the algorithm returns to the previous "best" model, if it exists, or a fixed threshold on the misfit based on a noise estimate, a typical value for which was found to be $\varepsilon_{threshold}=2.5\%$ (or the logarithm thereof).

The flexibility of the inversion scheme is one of its advantages and it is easy to accommodate other misfit functions, cooling schemes and search strategies than the ones described here. Neither the choice of frequencies nor the plane-layer model geometry is a limitation to the method, which can be extended to more complicated geometries with an appropriate forward code.

Results

We tested the inversion scheme on data from a single receiver in an SBL survey line crossing the Troll West Gas Field in the Norwegian Sea (Johansen et al., 2005). The Jurassic sandstone reservoir with a gas column of up to 160m lies 1100-1200m below the seafloor. The resistivity of the gas filled interval has been estimated from well-logs to be around 70Ωm, whereas the water bearing sands and overburden sediments have resistivities in the 0.5-2.0Ωm range. Other geological information from the area indicates a resistive basement at depths of about 5km below the seafloor. We chose to invert a receiver located at a water depth of 320m and above the edge of the reservoir. Thus, the in-towing data (source is towed towards the receiver) contain only information on the background geology/resistivities, whereas the out-towing data (source is towed away from the receiver) contain a strong contribution from the guided reservoir wave.

The inversion was run with and without the up-down separation step, yielding the results shown in figure 2 (for out-towing) and figure 3 (for in-towing). In all four cases, the base source frequency of 0.25Hz and its 3rd harmonic of 0.75Hz were considered. Higher harmonics were not included to ensure optimal data quality. A 14-layer formation was assumed. Layer thicknesses increase as a function of depth (from 100m at the top up to 890m at the bottom) with the deepest layer extending to infinity. We used a starting temperature T_0 of 2 and a decay factor C of 0.01 divided by the number of layers. The figures include plots of the best resistivity-depth profile obtained (left), the data misfit at each iteration (center), and a comparison of the amplitude and phase of the acquired data against the final synthetic data at 0.25Hz (right). The data fit at 0.75Hz exhibited very similar behavior.

From figure 2, we observe that the two inversions of the out-towing data produced very similar resistivity-depth profiles. The gas column is clearly visible, though slightly deeper than known from the well-logs. Below the gas
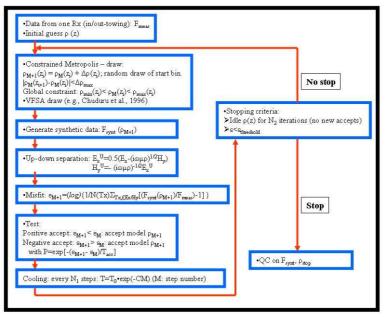

Figure 1: Flow chart the inversion scheme.

Inversion of marine CSEM data using up-down wavefield separation and simulated annealing

column, the resistivity returns to values between 1-2Ωm before starting to gradually increase at a depth of about 2.5km below the seafloor. This increase points to a resistive basement at depths below 5km, but may also be an indicator of resistive Triassic or Permian sediments. Note that our smoothness constraint ($\Delta\rho$<50Ωm between neighboring layers) clearly left an imprint on the resistivity-depth profiles obtained. Both resistivity profiles fit the data well. Looking at the center panels, which show how the data misfit evolves during the inversion, we find that the inversion with up-down separation was slightly slower in finding models reducing the misfit. We interpret this behavior as a result of a steeper and "rougher" misfit function, which can constrain the mobility of the model search when the cooling is slightly too fast at the critical temperature for the data at hand.

The benefit of using up-down separation in the inversion is much more apparent in the inversion results of the in-towing data, which are shown in figure 3. Again, the final data match is good in both cases (right panels), yet the inversion with up-down separation yielded a resistivity-depth profile much more consistent with the ones obtained from the out-towing data. Without up-down separation, the gradually increasing resistivity at great depths is not resolved. The different behavior is also evident from the evolution of the data misfit (center panels). Here, the misfit drops much sharper when up-down separation is used and leads to a final data misfit much lower than that achieved without (-3.33 vs. -2.94). In fact, without up-down separation, the model search became idle at iteration 11773, where it could not find neighboring models that reduce the misfit further, and stopped.

To verify that the inversion with up-down separation would have clearly excluded the resistivity-profile obtained without up-down separation, we recomputed the data misfit for the latter, but now including up-down separation, the result of which is listed in table 1. The attained data misfit value of -2.72 is well above the best model minimum of -3.33 obtained by the inversion with up-down separation. The latter had already passed the misfit level of -2.72 as early as iteration 8150. We can therefore be certain that the inversion with up-down separation would have excluded the resistivity-depth profile without the resistive basement. To complete the analysis, we also computed the data misfit without up-down separation for the best model obtained by the inversion with up-down separation (see table 1). This yielded a misfit of -3.09 which is only slightly lower than the best model minimum of -2.94 obtained by the inversion without up-down separation. The data misfit comparison summarized in table 1 clearly illustrates that including up-down separation in the inversion increases the sensitivity to weak, deep resistors in shallow-water environments.

Discussion

The inversion of the off-reservoir data (in-towing) benefited most from the inclusion of the up-down separation in the inversion scheme. Its inclusion was crucial for detecting the deeper resistive structures (> 2.5km below seafloor), whose response otherwise would have been masked by the air wave. In contrast, the inversion of the on-reservoir data (out-towing), exhibiting a strong reservoir response, did not produce different results when including/excluding the up-down separation. This indicates that the inclusion of the up-down separation in the inversion seems to work best in the case where it is needed most, i.e. in the presence of very weak resistive anomalies. This makes the procedure well suited for obtaining a background model for 3D inversion. Alternatively, background resistivity-depth profiles obtained by the 1D inversion scheme can be combined with bathymetry information to form a reference model for the interpretation of Scanning data. We feel that in the presence of a large hydrocarbon reservoir, up-down separation has a tendency to make the misfit function steeper and "rougher". Consequently, the cooling schedule and the search strategy employed in the simulating annealing become important design aspects of an efficient global inversion scheme with up-down separation.

It is important to note that the 1D examples presented here serve mainly to demonstrate the principle of using up-down separation in the inversion of marine CSEM data to increase sensitivity to weak resistive anomalies in shallow water environments. Up-down separation can equally be incorporated in higher dimensional inversion schemes.

Present work includes the parallelization of the algorithm, which is straightforward by running it with different random number seeds on a number of processes and estimating the average of the model ensemble. On one single processor, the inversion generally demonstrates good convergence after ~$8*10^3$ iterations with less than one second per step, depending on the number of harmonic frequencies included.

		Data misfit for best model	
		without up-down separation	with up-down separation
Inversion	without up-down separation	-2.94	-2.72
	with up-down separation	-3.09	-3.33

Table 1: Data misfit comparison for the models obtained from inverting the in-towing data (off-reservoir).

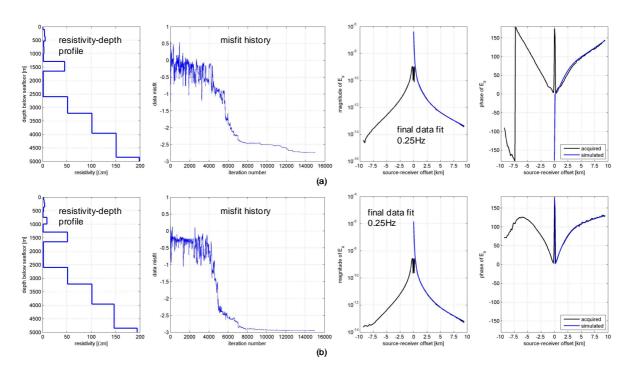# Inversion of marine CSEM data using up-down wavefield separation and simulated annealing

Figure 2: Inversion results for the out-towing data (on-reservoir): (a) with up-down separation, (b) without up-down separation.
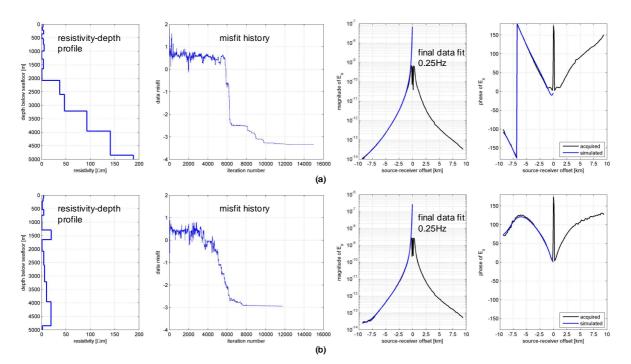

Figure 3: Inversion results for the in-towing data (off-reservoir): (a) with up-down separation, (b) without up-down separation.